CONF-9105-45--1

LA-UR -90-3634

LA-UR--90-3634

DE91 001856

Los Alamos National Laboratory is operated by the University of California for the United States Department of Energy under contract W-7405-ENG-36

TITLE NONINVASTIVE STUDIES OF HUMAN VISUAL CORTEX USING NEUROMAGNETIC TECHNIQUES

AUTHOR(S): C. J. Aine, J. S. George, S. Supek, P-6
E. L. Maclin, VA Medical Center, Albuquerque, NM

SUBMITTED TO: Optical Society of Amer.-Noninvasive Assessment of the Visual System, February 4-7, 1991

DISCLAIMER

Los Alamos National Laboratory
Los Alamos, New Mexico 87545

FORM NO 836 R4
ST NO 2629 5/81

Noninvasive Studies of Human Visual Cortex Using Neuromagnetic Techniques

C.J. Aine, J.S. George, S. Supek, and E.L. Maclin*

Physics Division, Mail Stop M715
Los Alamos National Laboratory, Los Alamos, NM 87545
*Center for Magnetoencephalography, VA Medical Center
Albuquerque, NM 87108

Introduction

The major goals of noninvasive studies of the human visual cortex are: (1) to increase knowledge of the functional organization of cortical visual pathways; and (2) to develop noninvasive clinical tests for the assessment of cortical function. Noninvasive techniques suitable for studies of the structure and function of human visual cortex include magnetic resonance imaging (MRI), positron emission tomography (PET), single photon emission tomography (SPECT), scalp recorded event-related potentials (ERPs), and event-related magnetic fields (ERFs). The primary challenge faced by noninvasive functional measures is to optimize the spatial and temporal resolution of the measurement and analytic techniques in order to effectively characterize the spatial and temporal variations in patterns of neuronal activity. In this paper we review the use of neuromagnetic techniques for this purpose.

Methods

Activation of human visual cortex by suitable visual stimuli produces magnetic fields that can be recorded outside the head using magnetic detectors comprised of sensor coils coupled to superconducting quantum interference devices (SQUIDs). Depending upon the specific coil configuration, such detectors act as first- or second-order gradiometers which produce a voltage output proportional to the first or second spatial derivative of the magnetic field oriented normal to the surface of the head. Neuromagnetic fields associated with cortical activity typically range from 10^{-12} to 10^{-14} tesla (T), compared to urban background noise of up to 10^{-6} T, and the earth's magnetic field of approximately 5×10^{-5} T. A neuromagnetic measurement system is illustrated schematically in **figure 1.**

Neuromagnetic measurements result in a spatial-temporal data matrix (magnetic field strengths at each of T time points for each of N recording sites). Determining the pattern of neuronal currents in the brain that give rise to an observed magnetic field pattern outside the head is termed the neuromagnetic *inverse problem.* Because a given magnetic field on the surface of the head could be due to any number of possible source configurations, the inverse problem has no unique solution. Approximate solutions are possible, however, if assumptions are made regarding the shape and conductivity of the head and the number and configuration of neuronal currents responsible for the surface distributions (Sarvas, 1987). Using this approach, numerical minimization techniques can be used to determine the best-fitting source or sources, subject to the assumptions of a particular model. This approach to the inverse problem becomes more attractive when solutions are further constrained by applying knowledge of brain physiology and anatomical structure to the source modeling procedures.

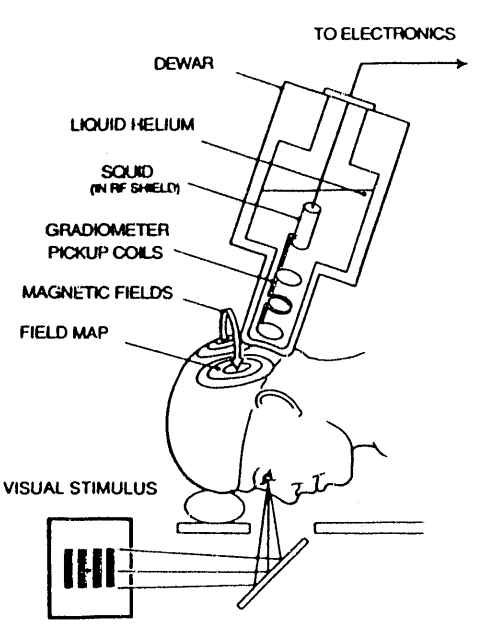

Figure 1. Experimental Setup.

The most commonly used source model for both magnetic and electrical data is a single point current dipole which represents the centroid of synchronous activity of a population of neurons (Kaufman et al., 1984; Wood, 1982). This model is applied to the field distribution at a single latency and yields the location, orientation, and strength of the current dipole that best accounts for the observed data in a least-squares sense. Such best-fitting current dipoles are *equivalent* in the sense that the magnetic field generated by a single current dipole is used as a simplified representation of fields generated by more complex source configurations. Multiple dipole models can be fitted using similar techniques when single dipole models are inadequate to account for the data. More advanced models under development by a number of investigators attempt to account for the entire spatial-temporal data matrix using a small number of spatially fixed dipoles with time-varying magnitudes.

Figure 2 illustrates the steps involved in deriving equivalent current dipoles (ECDs)

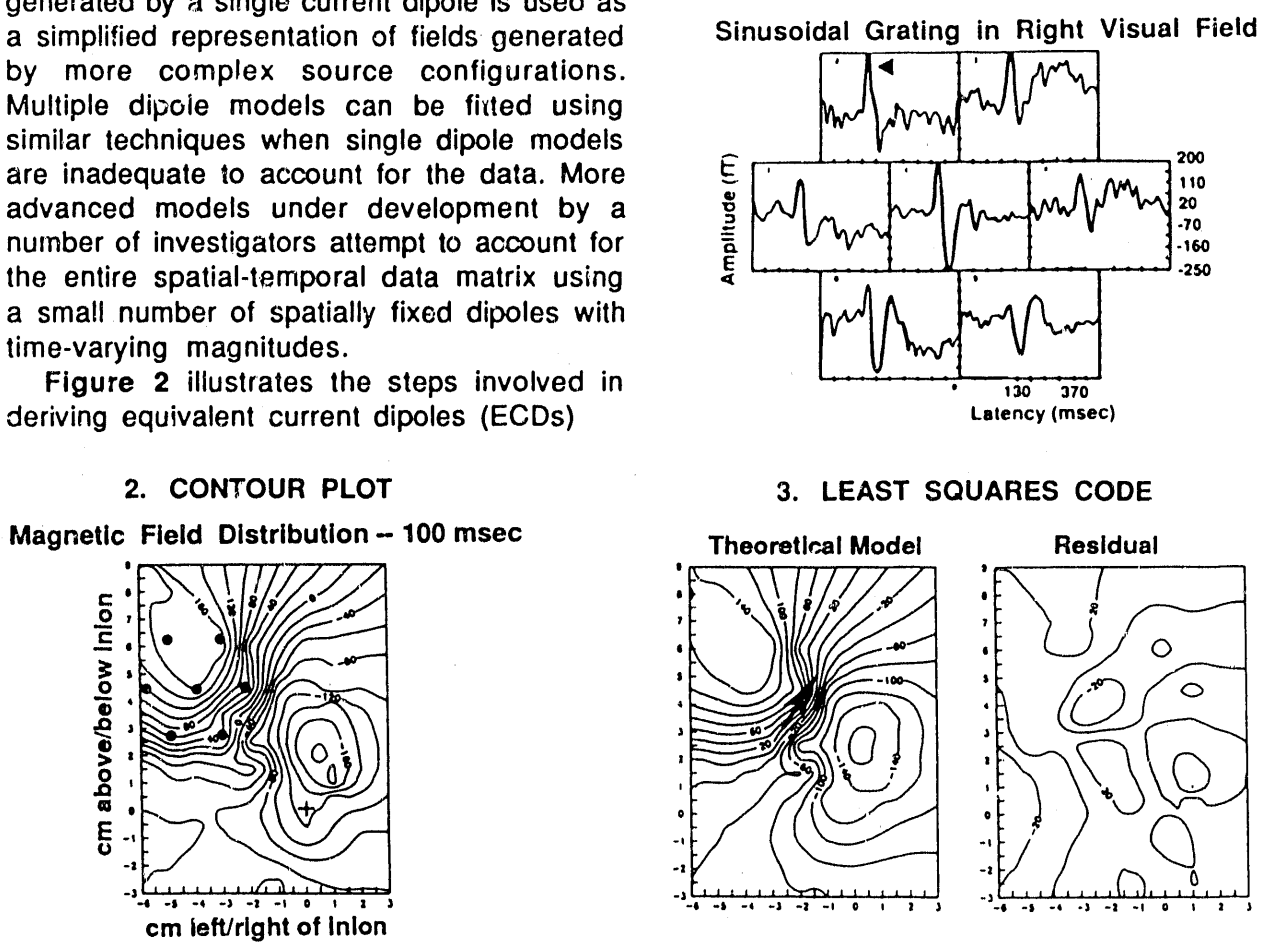

Figure 2. General procedures for data analysis. See text for explanation.

from magnetic field distributions. **Part 1** displays magnetic data from a single placement of a 7-channel hexagonal sensor array. During a given experiment, the 7-sensor array is moved to several locations over the surface of the head and the experimental conditions are repeated for each position of the array until the desired surface area is completely mapped. Field amplitudes are measured relative to a prestimulus baseline. Iso-amplitude maps, as shown in **Part 2**, are then contructed at individual latencies by interpolation and are displayed as contour or pseudocolor maps. Each contour line represents a region of equal magnetic field strength (positive values indicate magnetic flux out of the head, negative values into the head). One placement of the 7-sensor array is indicated by dots in the upper left of the contour map. In this field map the inion (the bony protrusion at the back of the head) is at x=0, y=0 (indicated by + on the map). Note the existence of a positive peak at x=-4.5, y=6.0 and a negative peak at x=0, y=2.0.

When the field maps demonstrate the existence of two primary extrema (i.e., a single pair of positive and negative peaks), the location, orientation, and strength of the best-fitting single current dipole are calculated using a nonlinear least-squares algorithm. **Part 3** illustrates the magnetic field generated by the best-fitting ECD for the empirical data shown in part 2, together with a map of the residual magnetic field strength unaccounted for by the single dipole model. This ECD is shown as an arrow on the contour map. In this case the ECD accounted for 94% of the total variance of the original data. Two and 3-dipole models are applied to the data if there is evidence of three or more extrema in the field distributions and/or the residual field maps contain a dipole-like field pattern. A comparison of single versus multiple dipole models can be made by examining reduced Chi-square (X_r^2) values associated with each model; values between 1.0 and 1.5 are interpreted as adequate fits to the data (e.g., Bevington, 1969). Monte Carlo simulations are performed to assess the stability of the model solutions with respect to noise and to determine whether source parameters differ significantly as a function of experimental conditions (Medvick et al., 1990).

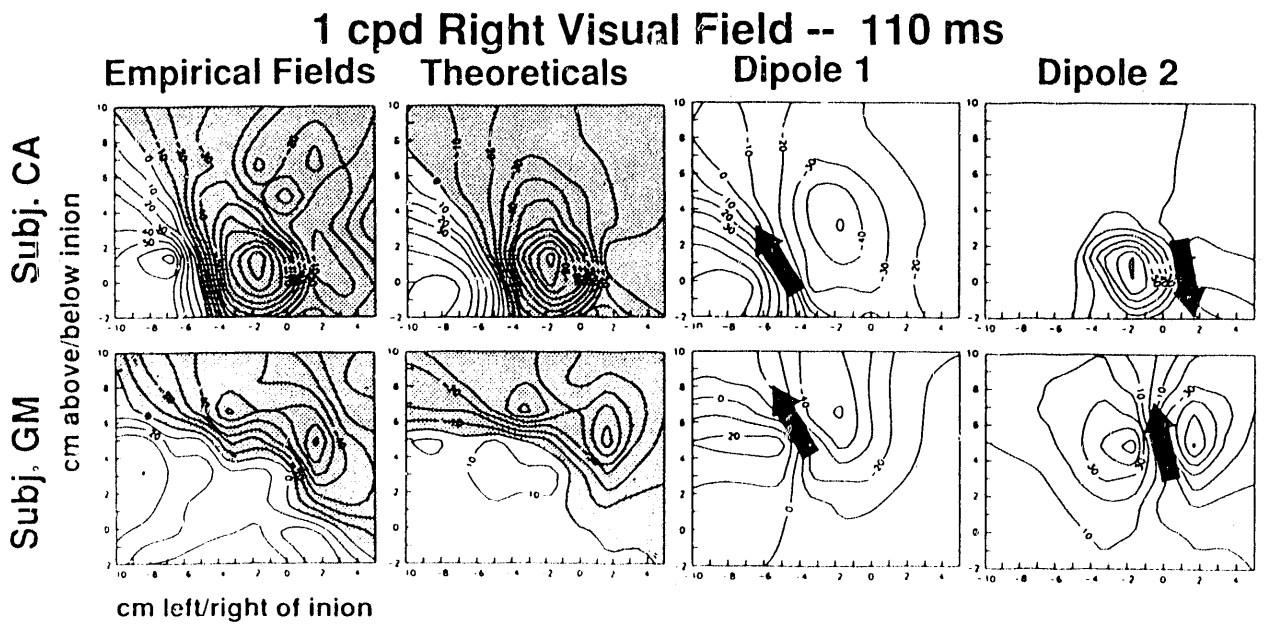

Figure 3. Empirical and 2-dipole theoretical distributions (first two columns) for two subjects show at least two sources at 110 msec when a 1 cpd grating was centered 7° along the horizontal meridian of the right visual field. Theoretical distributions are shown in columns 3 and 4 for the component dipoles (Dipole 1 and Dipole 2) obtained from the 2-dipole model.

In **Part 4** the coordinate system of the magnetic measurements and ECD model is transformed into that of MRI scans to permit determination of the locations of ECDs relative to anatomical structures (George et al., 1990). By radiological convention, MRI sections are displayed as though viewed from in front of or underneath the head so that the left hemisphere is displayed on the right side of the MRI section. Coordinate reconciliation is achieved by attaching oil-containing capsules to the head at designated reference locations to provide precise common fiducial marks in the two coordinate systems.

Field distributions characterized by a single dipole-like configuration are often observed in distributions reflecting early cortical activity (e.g., 70-100 ms) in response to visual stimulation. Later activity (> 100 ms) most often appears to be a composite of multiple sources with different time-courses. **Figure 3** displays such an example for two subjects. At least two ECDs can be fitted at 110 ms for both subjects when a 1 cpd grating was presented in the right visual field. These models were considered adequate since the X_r2 values for the 2-dipole model ranged from 1.13-1.5. The percent of variance accounted for by the 2-dipole models ranged from 75-77%. In comparison, X_r2 values for the single-dipole models ranged from 1.80-1.82 and the percent of variance ranged from 44-67%. A 3-dipole model was also considered adequate for GM's data (X_r2=1.0, percent of variance=77) which modeled an additional right hemisphere ECD (see the empirical fields at x=1.0, y=0). A similar right hemisphere ECD has been identified in CA's data at 120 ms. Although the field distributions for the two subjects appear quite different, the ECD solutions are more similar between subjects. One ECD is located along the midline (x=0) and the other is located lateral to the midline ECD in the left hemisphere (x=-5). The major difference between the ECDs across these subjects is the location along the y axis, which may be attributable to differences in cortical geometry between subjects (e.g., the relation of the calcarine fissure to the inion). Radically different field distributions can result from slight differences in orientation of two or more dipoles.

Conclusion

The primary challenge for noninvasive functional measurements is the spatial and temporal resolution of multiple sources. This paper has described ways in which neuromagnetic techniques have been applied toward this end. When complex field patterns are reduced to component sources, similarities across subjects are more apparent than in the field distributions themselves. By combining neuromagnetic measurements with manipulation of visual stimuli, it should be possible to characterize the normal and pathological function of cortical visual pathways.

References

Bevington, P.R. 1969: Data Reduction and Error Analysis for the Physical Sciences. New York: McGraw-Hill.

Fox, P.T., Miezin, F.M., Allman, J.M., Van Essen, D.C. and Raichle, M.E. 1987: J. Neurosci. 7:913-922.

George, J.S., Jackson, P.S., Ranken, D.M. and Flynn, E.R. 1990: In S.J. Williamson, M. Hoke, G. Stroink, and M. Kotani (eds.). Advances in Biomagnetism, New York: Plenum, pp. 737-740.

Kaufman, L., Okada, Y., Tripp, J. and Weinberg, H. 1984: Ann. N.Y. Acad. Sci., 425:722-436.

Maclin, E.L., Okada, Y.C., Kaufman, L. and Williamson, S.J. 1983: Il Nuovo Cimento. 2:410-419.

Medvick, P.A., Lewis, P.S., Aine, C. and Flynn, E.R. 1990: In S.J. Williamson, M. Hoke, G. Stroink, and M. Kotani (eds.). Advances in Biomagnetism, New York: Plenum, pp. 543-546.

Sarvas, J. 1987: Phys. Med. Biol., 32:11-22.

Wood, C.C. 1982: Ann. N.Y. Acad. Sci., 388:139-155.

END

DATE FILMED

01/08/91